

Parasitic-free measurement of the fundamental frequency response of a semiconductor laser by active-layer photomixing

Michael A. Newkirk and Kerry J. Vahala

Department of Applied Physics, 128-95, California Institute of Technology, Pasadena, California 91125

(Received 7 December 1987; accepted for publication 4 January 1988)

We report the measurement of the fundamental (intrinsic) frequency response of a GaAs semiconductor laser to 12 GHz by directly photomixing two optical sources in the active region of the laser. This novel technique reveals the underlying fundamental frequency response of the device as parasitic effects are avoided. Well beyond the relaxation resonance, the theoretically predicted 40 dB/dec signal rolloff is observed. Other features of the measured response function are also observed to be the theoretical ideal.

The frequency response of a semiconductor laser to direct modulation is important to many optical communication systems employing these devices as sources. The ultimate frequency limit for semiconductor laser modulation is determined by the electron-photon relaxation resonance frequency. The response function associated with this process is referred to as the fundamental or intrinsic response of the device.¹ Often, however, the maximum modulation bandwidth is reduced by the unavoidable parasitic impedances in packaged laser diodes. These parasitic elements limit ordinary carrier injection at high frequencies by shunting current from the active region. Even in high-speed laser structures, where parasitic effects are circumvented up to the relaxation resonance, they soon dominate the modulation behavior beyond the resonance, masking the fundamental response of the device.² An experimental technique to probe the fundamental modulation response of a laser diode is therefore important. In this letter we propose and demonstrate such a technique. In our system we photomix (i.e., heterodyne) two single-frequency laser sources directly in the active region of the device whose response is to be measured. The resulting modulation is thus independent of carrier transport, and parasitic effects are avoided. Previously, the photomixing technique has been used to measure the frequency response of photodetectors.^{3,4} In these cases, however, both the intrinsic device response and the parasitic response are measured simultaneously, since the photomix-generated signal is dependent upon current transport out of the device under test.

The intrinsic modulation response can be derived easily in the small signal limit by using the spatially averaged rate equations. The response function is given by¹

$$\frac{\hat{p}_m(\Omega)}{p_0} = \frac{\Gamma G' I_m(\Omega)}{\omega_R^2 - \Omega^2 + i\Omega\gamma}, \quad (1)$$

where p_0 is the steady-state lasing mode photon density, $\hat{p}_m(\Omega)$ is the corresponding small signal amplitude response function, Γ is the filling factor, G' is the derivative of the optical gain with respect to carrier density, $I_m(\Omega)$ is the injection level amplitude in units of carrier density per second, ω_R is the relaxation oscillation frequency, and γ is the relaxation oscillation damping rate. The intrinsic response function is therefore flat at low frequencies, has a resonance near ω_R , and rolls off rapidly with increasing frequency beyond this resonance. The rolloff in Eq. (1) of 20 dB/dec

translates into a 40 dB/dec rolloff in detected power from a photodetector. The relaxation resonance frequency ω_R is given by¹

$$\omega_R = \sqrt{G' p_0 / \tau}, \quad (2)$$

where τ is the photon lifetime. Much progress has been made in extending the intrinsic frequency response by increasing ω_R . This includes the use of window structures to increase p_0 (Ref. 5) and multiple quantum well active layers to increase G' .^{6,7} Verification of the intrinsic response at these frequencies is difficult, however, since great efforts must be made to reduce parasitic effects.

The photomixing technique involves the mixing of two laser beams with a small frequency difference in an absorbing medium. When the beams are mixed in a semiconductor, for example, the carrier density is modulated at the beat frequency. By varying the frequency of one or both lasers, the beat frequency can be tuned to encompass the entire microwave spectrum.

In our system we combine light from a krypton laser and a dye laser to generate the microwave modulation. The krypton laser, with an intracavity étalon, operates in a single longitudinal mode at 752.5 nm. The output power is approximately 250 mW. The single-mode ring dye laser, running with Pyridin 2 dye, generates 250 mW at the same wavelength. The light from these sources is focused into single-mode optical fibers and combined in a 50/50 fiber coupler that mixes the light. By stressing one input arm of the fiber coupler, we bring the polarizations of the two beams into alignment at the output, so that the maximum power is available for optical modulation. The beat frequency is controlled by tuning the dye laser, which can be electronically scanned over a 30 GHz range. The dye laser frequency is actively stabilized to 500 kHz, so that the stability of the beat frequency spectrum is determined by the stability of the krypton laser frequency, which we measure to be 10 MHz as a result of room microphonics. Initial overlap of the two frequencies is accomplished by first directing the output from one arm of the fiber coupler into a 0.75 m grating spectrometer and superimposing the two lines to within 40 GHz, the resolution of the instrument. We then illuminate a photodiode with the mixed light and scan the dye laser until the beat frequency falls within the bandwidth of the photodiode, appearing on an electronic spectrum analyzer. The dye laser scan offset is then adjusted until the beat frequency can be

continuously scanned from 0 to 30 GHz.

The device used in this experiment is a Mitsubishi GaAs transverse junction stripe (TJS) laser diode with a 16.2 mA lasing threshold and lasing wavelength of 838 nm. This particular device had a transparent contact to facilitate the photomixing process. It was mounted in a low-frequency hermetically sealed capsule that was disassembled for the experiment. As shown in Fig. 1, the mixing pump light is focused by a cylindrical lens and microscope objective to a stripe coincident with the active region. In this way we can couple uniformly into the active region over the entire length of the device. For alignment purposes the same microscope objective images the top surface of the laser diode on an infrared vidicon. Both luminescence from the active region and reflected pump light are visible on the monitor, making rough alignment possible. Maximum coupling is achieved by peaking the laser modulation signal detected on a *p-i-n* photodiode (Ortel PD050-OM). An optical isolator suppresses feedback to the laser diode and rejects any scattered pump light going to the detector. The detected microwave photocurrent was measured with an HP 8565A spectrum analyzer combined with an HP 8349B amplifier. We calibrated the system—detector, amplifier, and cables—to 20 GHz using the photomixing technique directly on the detector.

The beat frequency power incident on the active region of the semiconductor laser is approximately 7 mW, which takes into account a 30% Fresnel reflection from the contact layer. By optimizing the pump optics, this figure has been improved substantially since this experiment was completed. The intensity modulation of the semiconductor laser output can be found from the ratio of the amplitude of the rf

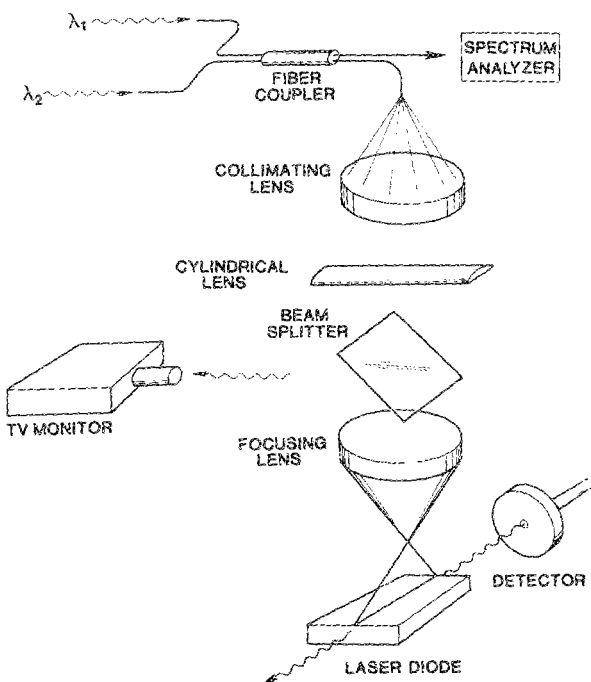


FIG. 1. Schematic diagram of the experimental arrangement.

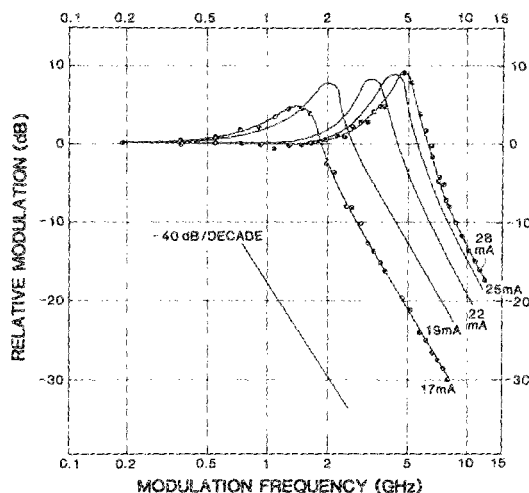


FIG. 2. Measured modulation response at different bias levels. The response peaks and 40 dB/dec rolloff are clearly visible, indicating the absence of parasitic effects.

photocurrent to the dc photocurrent. The modulation index is 5.6% and 10.3%, well below the resonance for a 28 and 22 mA bias, respectively. Further increases in the beat frequency pump power thus offer the possibility of modulating the output intensity at fairly high levels.

Plots of the observed modulation response in relative units at different bias currents appear in Fig. 2. Data points are only given on two curves for clarity. We note the resonances are clearly defined. For each curve we also observe the ideal 40 dB/dec rolloff well beyond the resonance. This is most easily seen on the 17, 19, and 22 mA curves, where the data extend to several multiples of the resonance frequency. By use of Eq. (1), we can extract from these curves ω_R and γ for each bias level. A plot of ν_R^2 versus injection current appears in Fig. 3 and exhibits the theoretical linear behavior for above threshold operation. The damping rate γ can be expressed as

$$\gamma = \gamma_0 + \tau\omega_R^2, \quad (3)$$

where γ_0 includes the power independent sources of damp-

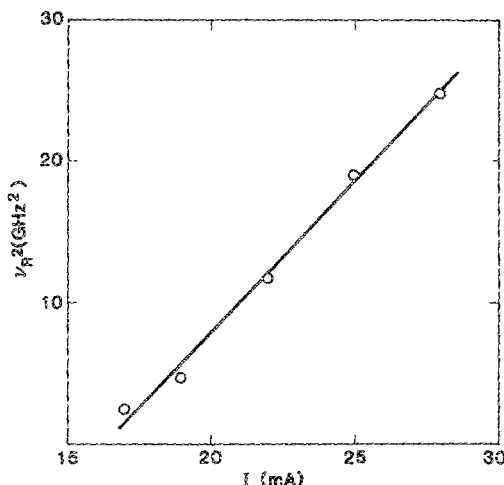


FIG. 3. Square of resonance frequency vs bias current.

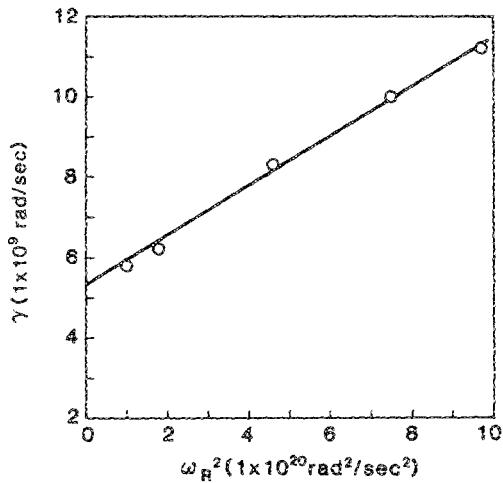


FIG. 4. Damping rate γ vs ω_R^2 . The ideal linear relationship is predicted by Eq. (3).

ing (e.g., spontaneous emission, diffusion, etc.). The expected linear relationship between γ and ω_R^2 is verified in Fig. 4. The slope and intercept of the resulting line yield estimates for γ_0 and τ of $5.3 \times 10^9 \text{ rad s}^{-1}$ and 6.2 ps, respectively. From these results we infer that the measured modulation response curves are close to ideal, free of any parasitic influences.

In conclusion, we have measured the intrinsic modulation response of a TJS laser diode by photomixing two lasers directly in the active region of the device. The response curves appear to be ideal, since there is no indication of any parasitic effects. We look forward to extending the technique to investigate the intrinsic modulation response of high-speed laser structures.

This work was supported by the National Science Foundation, the Powell Foundation, and AT&T Bell Laboratories. The authors are grateful for stimulating conversations with Joel Paslaski.

- ¹K. Y. Lau, N. Bar-Chaim, I. Ury, Ch. Harder, and A. Yariv, *Appl. Phys. Lett.* **43**, 1 (1983).
- ²C. B. Su, V. Lanzisera, W. Powazinik, E. Meland, R. Olshansky, and R. B. Lauer, *Appl. Phys. Lett.* **46**, 344 (1985).
- ³H. Blauvelt, G. Thurmond, J. Parsons, D. Lewis, and H. Yen, *Appl. Phys. Lett.* **45**, 195 (1984).
- ⁴S. Kawanishi and M. Saruwatari, *Electron. Lett.* **22**, 337 (1986).
- ⁵K. Y. Lau, N. Bar-Chaim, I. Ury, and A. Yariv, *Appl. Phys. Lett.* **45**, 316 (1984).
- ⁶Yasuhiko Arakawa, Kerry Vahala, and Amnon Yariv, *Appl. Phys. Lett.* **45**, 950 (1984).
- ⁷K. Uomi, T. Mishima, and N. Chinone, *Appl. Phys. Lett.* **51**, 78 (1987).